

# Characterization and Crystallization of Soluble Human Fcγ Receptor II (CD32) Isoforms Produced in Insect Cells<sup>†</sup>

Peter Sondermann,<sup>\*,‡,§</sup> Uwe Jacob,<sup>||</sup> Claudia Kutscher,<sup>§</sup> and Jürgen Frey<sup>§</sup>

Max-Planck-Institut für Biochemie, Abt. Strukturforschung, Am Klopferspitz 18a, D-82152 Martinsried, Germany, and Universität Bielefeld, Fakultät für Chemie, Biochemie II, 33615 Bielefeld, Germany

Received December 8, 1998; Revised Manuscript Received April 21, 1999

**ABSTRACT:** FcγRII (CD32), the receptor for the Fc part of IgG, is responsible for the clearance of immunocomplexes by macrophages and plays a role in the regulation of antibody production by B cells. To investigate the process of immunocomplex binding in terms of stoichiometry and stability of the FcγRII: IgG complex, we produced both FcγRII isoforms (FcγRIIa and FcγRIIb) as soluble proteins in insect cells. The expressed proteins could be purified in high yields and were biologically active as judged by their ability to bind IgG. Thus, the minor glycosylation performed by the insect cells is not crucial for the binding of the usually highly glycosylated FcγRII to IgG. The dissociation constant of the sFcγRIIa: IgG-hFc complex was determined by fluorescence titration ( $K_D = 2.5 \times 10^{-7}$  M). Complementary sFcγRIIa antagonizes immunocomplex binding to B cells. Here sFcγRIIa showed a comparable dissociation constant ( $K_D = 1.7 \times 10^{-7}$  M) which was almost 10-fold lower than the constant for FcγRIIb. The stoichiometry of the FcRIIa:IgG-hFc complex was determined by equilibrium gel filtration and shows that IgG is able to bind alternatively one or two FcγRII molecules in a noncooperative manner. Furthermore, in an ELISA-based assay the isotype specificity of various anti-FcγRII monoclonal antibodies was measured as well as their ability to interfere with the IgG recognition through its receptors. To further investigate the molecular basis of the FcγRII–ligand interaction, we crystallized FcγRIIb. Trigonal crystals diffracted to 3 Å and the structure solution is in progress.

Fc receptors for IgG (FcγR)<sup>1</sup> have been a focus of interest for many years due to their crucial role in the human immune system (1–4). These type I transmembrane proteins are expressed in a specific pattern on all immunocompetent cells. The family of FcγRs is comprised of three members: The extracellular part of FcγRI (CD64) consists of three immunoglobulin-like domains, whereby the third domain is responsible for the higher affinity to IgG in comparison to the other two members, FcγRII (CD32) and FcγRIII (CD16), which possess only two extracellular Ig-like domains. While the extracellular repeats of these proteins are very homologous, the cytoplasmic regions responsible for triggering effector functions show no relation to each other.

FcγRs are involved in the clearance of immunocomplexes, the antibody-dependent cellular cytotoxicity (ADCC), the secretion of mediators, and the regulation of B cell proliferation and differentiation. FcγRII which is expressed on nearly all immunocompetent cells is primarily responsible for mediating phagocytosis of immunocomplexes. The extracellular part of this protein can be one of two isoforms, FcγRIIa and FcγRIIb, which differ in only 7% of their amino acid residues. Nevertheless, the affinity to IgG subclasses varies clearly between both isoforms.

Soluble FcγRs (sFcγRs) were termed after their discovery as “immunoglobulin binding factors” (5). The most common way the cell generates sFcγRs is by proteolysis of the membrane-bound form which is observed for sFcγRII (6, 7) and sFcγRIII (8). sFcγRII can also be produced by alternative splicing of the hnRNA, as demonstrated for sFcγRIIa (9). Finally separate genes code for the two soluble forms of FcγRI (4). Thus, the release of sFcγRs seems to be controlled by the organism. In vitro experiments showed that human Langerhans cells respond with increased release of sFcγRIIa after stimulation with TNF-α (10). Although it could be shown that sFcγR inhibits antibody production in mice (11), the mechanisms of the sFcγR immunoregulative potential remain unclear. It is supposed that these soluble receptors represent a ligand for another membrane-bound molecule (eventually CR3) which mediates these immunosuppressive effects (12–14).

Recently the association of both the membrane-bound and the soluble form of FcγRs with several diseases has become evident. The membrane-bound forms are employed by Dengue virus (15) and HIV (16) to gain or enhance access

<sup>†</sup> This work was supported by the Deutsche Forschungsgemeinschaft (Graduiertenkolleg “Zelluläre Grundlagen biotechnischer Prozesse” and Sonderforschungsbereich 223).

<sup>\*</sup> To whom correspondence should be addressed.

<sup>‡</sup> Present address: Max-Planck-Institut für Biochemie, Abt. Strukturforschung, Am Klopferspitz 18a, D-82152 Martinsried, Germany. Telephone: 49-89-8578-2701. Fax: 49-89-8578-3516.

<sup>§</sup> Universität Bielefeld.

<sup>||</sup> Max-Planck-Institut für Biochemie.

<sup>1</sup> Abbreviations: ADCC, antibody-dependent cellular cytotoxicity; ahIgG, heat-aggregated human IgG; ATCC, American Type Culture Collection; ELISA, enzyme-linked immunosorbent assay; ESI-MS, electrospray ionization mass spectroscopy; FACS, fluorescence-activated cell sorter; FcγR, receptor for the Fc part of IgG; FCS, fetal calf serum; FITC, fluorescein isothiocyanate; FPLC, fast protein liquid chromatography; hFc, Fc fragment of human IgG; hIgG, human IgG; HPLC, high-performance liquid chromatography; IgG, immunoglobulin G;  $K_D$ , dissociation constant; mAb, monoclonal antibody; MES, 3-(morpholino)ethanesulfonic acid; MOI, multiplicity of infection; MOPS, 3-(morpholino)propanesulfonic acid; X-Gal, 5-bromo-4-chloro-3-indolyl-β-D-galactopyranoside.

to immune cells while the Ebola virus suppresses the activation of neutrophils by directly blocking Fc $\gamma$ RIII (17). The Measles virus nucleocapsid protein was demonstrated to bind to Fc $\gamma$ RII on B cells, which results in a suppression of antibody production (18). Furthermore, the serum concentration of sFc $\gamma$ Rs correlates with the stage of some autoimmune diseases such as systemic lupus erythematosus (SLE, 19) and rheumatoid arthritis (RA, 20), multiple myeloma (MM, 21), and HIV infection (22), making them a potential marker for the immune status of affected patients. In the case of MM, a therapy with sFc $\gamma$ R seems possible. After incubation of IgG-secreting myeloma cells with sFc $\gamma$ RIII, Hoover et al. reported a decrease in antibody production and after prolonged treatment lysis of cells (23).

To investigate the properties of sFc $\gamma$ Rs emphasizing the differences between human sFc $\gamma$ RIIa and sFc $\gamma$ RIIb, we produced both isoforms in insect cells employing recombinant baculoviruses. Our main focus was the stoichiometry of IgG binding, the respective dissociation constants, and the overall purity and homogeneity of the sFc $\gamma$ Rs sufficient to enter the structure solution process by X-ray crystallography.

## MATERIALS AND METHODS

**Cell Lines, Antibodies, and Reagents.** SF9 insect cells (24, ATCC CRL-1711) were grown in TC100 (Gibco) supplemented with 5% FCS. Daudi cells (ATCC CCL-213), a human B lymphoblast cell line, were maintained in RPMI 1640/10% FCS. BHK-21 cells (ATCC CCL-10) were cultured in DMEM/10% FCS and transfected as described (25). For homologous recombination, the isolated DNA of *Autographa californica* nuclear polyhedrosis virus (AcNPV, ATCC VR-1345, 26) was used. SDS-PAGE was performed according to Laemmli (27). hIgG-Sepharose was prepared by coupling hIgG from healthy donors (Centeon Pharma GmbH, Marburg, Germany) to 50 mg/mL drained resin of CNBr-activated Sepharose 4B (Sigma, Deisenhofen, Germany) according to the instructions of the manufacturer. The hFc (Centeon Pharma GmbH, Marburg, Germany) was produced from IgG of healthy donors and shows the normal distribution of subclasses. The enzyme used for removing N-glycosylation was PNGase F (NEB, Schwalbach, Germany). mAbs IV.3 (ATCC HB217, 28), AT10 (29), and KB61 (30) were obtained from the Fifth International Workshop on Human Leukocyte Differentiation Antigens; CIKM5 was obtained from Silenus Laboratories, Hawthorn, Australia, while 1A4.A, ID2.7, II1A5, and II8D2 were produced in the authors laboratory (31).

**Generation of Recombinant Baculoviruses.** The cDNAs of human Fc $\gamma$ RIIa, kindly provided by Dr. B. Seed (Department of Molecular Biology, Massachusetts General Hospital, Boston, MA), and human Fc $\gamma$ RIIb2, isolated from a placental cDNA library as described (32), were cloned into a pUC18 plasmid as template for mutagenesis by PCR. Fc $\gamma$ R-specific primers (Fc $\gamma$ RIIa, 5'-GGGCAGCAGCTGACCAATGGGGG-3'; Fc $\gamma$ RIIb2, 5'-GGGGATCATTAGGCTGTCGACAC-TGGG-3') were used in combination with M13 sequencing or reverse sequencing primer to amplify the part coding for the extracellular domain with the introduction of a stop codon (underlined) between the regions coding for the extracellular and the potential transmembrane part. By this procedure, sFc $\gamma$ RIIa was terminated after amino acid 177 and sFc $\gamma$ RIIb

after residue 180. The introduced mutations were verified by sequencing both strands with the dideoxy termination method (33). The mutated cDNAs were inserted downstream of the polyhedrin promoter region into the baculovirus transfer vector pA2 kindly provided by A. Hayes (Hoffmann-La Roche Ltd., Basel, Switzerland). The vector contains, beside the polyhedrin promoter region, a  $\beta$ -galactosidase gene for detection of the recombinant clones with the chromogenic substrate X-Gal. The cotransfection with AcNPV-DNA was performed as described elsewhere (34). Briefly, a 35 mm dish seeded with a monolayer of SF9 cells was incubated with a mixture of 500 ng of AcNPV-DNA, 2.5  $\mu$ g of transfer vector, and an equal volume of prediluted Lipofectin (2 parts with 1 part of sterile water; Life Technologies, Inc., Eggenstein-Leopoldshafen, Germany) in 1 mL of TC100 without FCS and maintained in a humidified atmosphere at 28 °C. After 5 h, 1 mL of TC100/5% FCS was added to the dish, and the supernatant was harvested after 48 h. The recombinant viruses were isolated by limiting dilution. Therefore, wells A1–H1 of a microtiter plate were filled with 100  $\mu$ L of the harvested supernatant subsequently diluted 1:1 in TC100/5% FCS. In a second step, row 1 with the diluted supernatant (A1–H1) was also diluted by 50% per row up to row 12 (A12–H12), resulting in identical dilutions in the diagonals of the plate. Then 100  $\mu$ L of SF9 cells (10<sup>6</sup>/mL) in TC100/5% FCS containing 1.5  $\mu$ L of a solution of 2% X-Gal in DMF was added to each well. After 5–7 days, the wells with recombinant viruses were identified by their blue color. This procedure was repeated with the supernatant of the positive well which contained the highest dilution of the virus suspension until the recombinant virus was homogeneous as judged by the absence of polyhedrin from infected cells.

**Production and Purification of the Recombinant Soluble Fc $\gamma$ RII.** SF9 cells were cultivated in a 1000 mL Superspinner (35) at a density of 10<sup>6</sup> cells/mL in TC100/5% FCS. Four days after infection with a MOI of 10, the supernatant was harvested and 1/20th volume of 1 M Tris/HCl, pH 8.0, was added. The ice-cold medium was centrifuged at 10000g for 30 min to remove the precipitated salt and was subsequently applied to a hIgG-Sepharose column. After extensive washing with 50 mM Tris/HCl, pH 8.0, followed by 10 mM Tris/HCl, pH 8.0, the column was eluted with 100 mM glycine/HCl, pH 3.0. The eluate was immediately neutralized with 1 M Tris/HCl, pH 8.0. The fractions containing the recombinant proteins were concentrated and subjected to gel filtration chromatography on a Superdex75 column (Pharmacia, Freiburg, Germany) preequilibrated with 150 mM NaCl, 2 mM MOPS/NaOH, 3 mM sodium azide, pH 7.0.

**Determination of the Protein Concentration.** The protein concentration was determined according to Gill and von Hippel (36). Briefly, the extinction coefficient at 280 nm of the denatured proteins was calculated from the amino acid sequence with all Cys residues appearing as half-cystines ( $\epsilon_{\text{hFc}} = 69\,280\text{ M}^{-1}\text{ cm}^{-1}$ ;  $\epsilon_{\text{sFc}\gamma\text{RIIa}} = 28\,120\text{ M}^{-1}\text{ cm}^{-1}$ ;  $\epsilon_{\text{sFc}\gamma\text{RIIb}} = 29\,400\text{ M}^{-1}\text{ cm}^{-1}$ ). These calculated values were employed to determine the protein concentrations in 6 M guanidinium chloride, 20 mM sodium phosphate, pH 6.5. The measured protein concentrations were used to obtain the extinction coefficients at 280 nm of the native proteins in PBS ( $\epsilon_{\text{hFc}} = 67\,940\text{ M}^{-1}\text{ cm}^{-1}$ ;  $\epsilon_{\text{sFc}\gamma\text{RIIa}} = 26\,670\text{ M}^{-1}\text{ cm}^{-1}$ ;  $\epsilon_{\text{sFc}\gamma\text{RIIb}} = 27\,880\text{ M}^{-1}\text{ cm}^{-1}$ ).

**Equilibrium Gel Filtration (Modified after Hummel and Dreyer, 37).** A 16/60 Superdex75 column (Pharmacia, Freiburg, Germany) connected to a FPLC station and calibrated with reference proteins was used. Afterward the column was equilibrated with hFc-containing buffer (150 mM NaCl, 2 mM MOPS/NaOH, pH 7.0, 3 mM sodium azide, and 7.1  $\mu$ M hFc). Then 6.0 nmol of sFc $\gamma$ RII was dissolved in the hFc-containing buffer and subjected to gel filtration. The retention time of the complex points to its mass while the integral of the negative peak (resulting from the hFc consumed from the column buffer for complex formation) relates to the stoichiometry of the complex.

In a second set of experiments, a PC3.2/30 Superdex75 column (Pharmacia, Freiburg, Germany) was equilibrated with a solution containing sFc $\gamma$ RIIa (150 mM NaCl, 2 mM MOPS/NaOH, pH 7.0, 3 mM sodium azide, and 0.600  $\mu$ M sFc $\gamma$ RIIa). Various amounts of sFc $\gamma$ RIIa were added to 4.5 pmol of hFc, solved in the equilibration buffer, and subjected to gel filtration. As in the previous experiment, the integral of the peak resulting from the sFc $\gamma$ RIIa consumed from the equilibration buffer for complex formation relates to the stoichiometry of the formed complex.

Both columns were calibrated with sFc $\gamma$ RIIa and hFc to relate the measured integrals to the injected protein concentration.

**Determination of the Dissociation Constants by Fluorescence Spectroscopy.** A solution of hFc was placed in a microcuvette (1.5 mL,  $1.68 \times 10^{-7}$  M or  $5.59 \times 10^{-7}$  M hFc in PBS) equipped with a magnetic stirring bar. sFc $\gamma$ RIIa (40  $\mu$ L,  $4.45 \times 10^{-5}$  M sFc $\gamma$ RIIa in PBS) was added with a calibrated multistep syringe (Hamilton, Bonaduz, Switzerland) in aliquots of 1  $\mu$ L. After each addition a fluorescence spectrum (20 °C, 300–350 nm) was recorded with a LS50B fluorescence spectrometer (Perkin-Elmer, Überlingen, Germany) using an excitation wavelength of 280 nm. The contribution of sFc $\gamma$ RIIa to the fluorescence was recorded in a second experiment under the same conditions without the hFc.

The fluorescence spectra of the isolated components, sFc $\gamma$ RIIa and hFc, were subtracted from the spectrum of the complex, revealing a maximum of the fluorescence difference signal at 327 nm.  $\Delta F_{327 \text{ nm}}$  values were obtained by correcting the signal from each spectrum of the complex in the fluorescence titration experiment at 327 nm for the contribution of the hFc and the sFc $\gamma$ RIIa. The dissociation constant ( $K_D$ ) was calculated by fitting it together with  $\Delta F_{\text{max}}$  (using an equation derived from the law of mass effects) to the  $\Delta F_{327 \text{ nm}}$  values and the corresponding sFc $\gamma$ RIIa concentrations:

$$\Delta F_{327 \text{ nm}} = (\Delta F_{\text{max}}/[L]_t n) [A - \sqrt{A^2 - [L]_t n [R]_t}]$$

where

$$A = ([R]_t + [L]_t n + K_D)/2$$

( $[L]_t$  = total concentration of hFc,  $[R]_t$  = total concentration of sFc $\gamma$ RIIa,  $\Delta F_{\text{max}} = \Delta F_{327 \text{ nm}}$  of the complex at infinite sFc $\gamma$ RIIa concentration,  $n$  = number of hFc binding sites for sFc $\gamma$ RIIa,  $K_D$  = dissociation constant of the sFc $\gamma$ RIIa:hFc complex).

**Inhibition of ahIgG Binding to Daudi Cells by sFc $\gamma$ RII Isoforms.** A human B lymphoblast cell line (Daudi) expresses Fc $\gamma$  receptors and consequently binds ahIgG. The potential of the recombinant sFc $\gamma$ RIIs to compete with the cell-expressed Fc receptors for ahIgG was tested. Therefore, varying concentrations of the sFc $\gamma$ RII isoforms (0–3.3  $\mu$ M) were preincubated for 20 min in 100  $\mu$ L of RPMI/10% FCS with 3  $\mu$ g of ahIgG (32) and were added to  $3 \times 10^5$  Daudi cells.

After incubating for 30 min on ice, the cells were washed with 1 mL of RPMI/10% FCS and precipitated by centrifugation (400g, 4 °C, 5 min). Then 100  $\mu$ L of FITC-labeled goat anti-human antibody (Dianova, Hamburg, Germany) were added. After incubation for 30 min on ice, the cells were washed (RPMI/10% FCS) and subjected to flow cytometry (FACSsort, Becton Dickinson, Heidelberg, Germany). The median value of the fluorescence for 10 000 counted cells was determined for each sample. The data were evaluated as percent inhibition between cells not incubated with sFc $\gamma$ R (0% inhibition) and cells that were not incubated with ahIgG and sFc $\gamma$ R (100% inhibition).

Finally, these experiments resulted in 8 data pairs of percent inhibition values with their corresponding concentrations of sFc $\gamma$ RII isoforms. To these data we fitted the dissociation constant and the concentration of active ahIgG using a modification of the formula described in the fluorescence titration experiment:

$$\% \text{ inhibition} = (100/[L]_t n) [A - \sqrt{A^2 - [L]_t n [R]_t}]$$

where

$$A = ([R]_t + [L]_t n + K_D)/2$$

( $[L]_t$  = concentration of active hIgG,  $[R]_t$  = total concentration of sFc $\gamma$ RII isoform,  $n$  = number of IgG binding sites for sFc $\gamma$ RII isoforms,  $K_D$  = dissociation constant of the sFc $\gamma$ RII:IgG complex).

**ELISA for Characterization of Anti-CD32 Antibodies.** The specificity of anti-CD32 antibodies for Fc $\gamma$ RII isoforms was measured as follows: the microtiter plate was incubated with 120 ng of sFc $\gamma$ RIIa/b per well (in 100  $\mu$ L of PBS, 20 °C, 12 h). The plate was washed and incubated with blocking buffer (PBS/0.2% Tween20, 30 min). An excess of the respective anti-CD32 mAb was added (100  $\mu$ L, 90 min). The plate was washed with blocking buffer before the peroxidase-labeled goat-anti mouse IgG+IgM antibody (Dianova, Hamburg, Germany) was added. After incubating for 90 min and subsequent washing with blocking buffer, 100  $\mu$ L of substrate buffer [0.2 M citrate/phosphate buffer, pH 5.2, 4 mg/mL *o*-phenylenediamine, 0.024% (v/v) hydrogen peroxide] was applied to the wells. The reaction was stopped by adding 50  $\mu$ L of 8 N sulfuric acid, and the absorbance at 490 nm was measured in an ELISA reader (Dynatech, Burlington, MA).

In a modified ELISA, the ability of the mAbs to interfere with the recognition of IgG by sFc $\gamma$ RIIs was measured. A microtiter plate was incubated with 15  $\mu$ g of hIgG per well (in 100  $\mu$ L of PBS, 4 °C, 12 h). After washing and blocking as described above, the plate was incubated with 230 ng of the respective Fc $\gamma$ RII isoform (90 min, 100  $\mu$ L of blocking



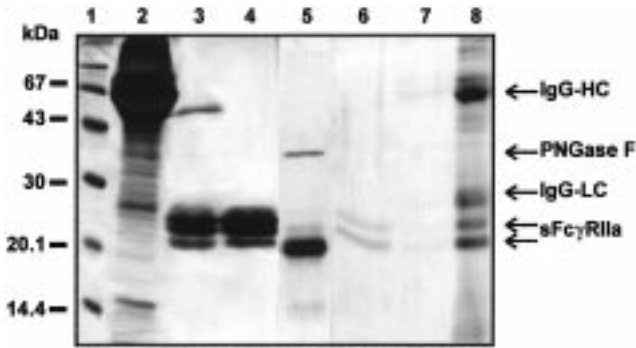


FIGURE 1: Purification and deglycosylation of sFcγRIIa derived from insect cells. Silver stain of a 15% reducing SDS-PAGE gel. Lane 1: Protein markers. Lane 2: Culture supernatant of infected SF9 cells. Lane 3: hIgG-Sepharose eluate after incubation with culture supernatant from lane 2. Lane 4: Concentrated hIgG-Sepharose eluate after size-exclusion chromatography. Lane 5: PNGase F (38 kDa)-treated protein before hIgG spin column. Lane 6: Partially deglycosylated sFcγRIIa. Lane 7: Effluent of a sample of lane 6 from a hIgG spin column. Lane 8: Laemmli eluate of the hIgG spin column. Some of the visible proteins are indicated by arrows (HC, heavy chain; LC, light chain).

buffer). The development of the assay was continued with the incubation of the anti-CD32 mAbs as described above.

All ELISAs were carried out in four independent experiments and the results corrected for the contribution of the respective mouse control IgG.

**Crystallization of Soluble sFcγRII Isoforms and Subsequent Data Collection.** The concentrated sFcγRII isoforms (11 mg/mL dissolved in 2 mM MOPS/NaOH, 150 mM NaCl, 3 mM sodium azide, pH 7.0) were crystallized in sitting drops (3 μL of protein solution + 1.5 μL of reservoir solution) at 293 K using the vapor diffusion method. Crystallization conditions which provided crystals were improved by varying pH, salt, precipitant, and additives. Diffraction data were collected on an image plate system (MAR Research, Hamburg, Germany) using graphite-monochromated CuKα radiation from a RU200b rotating-anode generator (Rigaku, Japan) operated at 50 kV and 100 mA. The reflections were integrated with the program MOSFLM (38), and subsequently the data were scaled, reduced, and truncated to obtain the structure-factor amplitudes using routines from the CCP4 program suite (39).

**RESULTS**

**Expression of Truncated FcγRII in Insect Cells and Their Biochemical Characterization.** To express active sFcγRII, a stop codon was inserted into the respective cDNA between the extracellular domain and the putative transmembrane region. These constructs were inserted into a baculovirus transfer plasmid and cotransfected with AcNPV DNA into SF9 cells. The recombinant virus was used for the infection of SF9 cells in suspension culture, which produced 2–4 mg of sFcγRII per liter of culture supernatant. The protein was enriched by affinity chromatography on a hIgG column (Figure 1). Residual IgG coeluting from the column was removed by gel filtration. Fractions of the purified receptors were subjected to SDS-PAGE, which revealed several bands due to heterogeneous glycosylation at a molecular mass of 20–23 kDa. Treatment of the receptors with PNGase F resulted in a single band with an apparent molecular mass

Table 1: Amino Acid Sequences Derived from Expressed sFcγRIIa and sFcγRIIb by N-Terminal Sequencing

	Eukaryotic signal peptidase ↓
FcγRIIa, unprocessed	ADSQAA APPKAVLKLE
FcγRIIb, unprocessed	VAGTPA APPKAVLKLE
BHK-21 derived sFcγRIIa	APPKAVL
Baculo derived sFcγRIIa	AA APPKA A APPKAV APPKAVL
Baculo derived sFcγRIIb	TPA APPKK A APPKAV

of 20 kDa (Figure 1). The glycosylation of both receptors was found to be mainly uncharged since their isoelectric point remained constant after deglycosylation (data not shown). The glycosylation of the receptors is not essential for IgG binding. Partially deglycosylated sFcγRII was spun through a hIgG mini column. The effluent and a eluate of the hIgG-Sepharose with Laemmli buffer showed that both forms bind to the column regardless of their glycosylation state (Figure 1).

N-Terminal sequencing of the purified sFcγRII isoforms revealed that insect cells can process mammalian signal sequences but the insect cell peptidase cuts at different sites, yielding a heterogeneous product. In contrast, the mammalian cell line BHK-21, transfected with the same construct, processes the protein uniformly (Table 1).

**Stoichiometry of the sFcγRII:IgG Complex.** Because of the low affinity of IgG to sFcγRII, a preformed complex cannot be isolated by size-exclusion chromatography. We attempted to investigate the stoichiometry of the complex with equilibrium size exclusion chromatography. Therefore, a column was equilibrated with hFc (50 kDa) dissolved in the running buffer. sFcγRIIa (22 kDa) was dissolved in this buffer and the mixture applied to the column. The complex remains formed due to the excess of hFc dissolved in the running buffer. The retention time/ $A_{280\text{ nm}}$  record (Figure 2a) showed a positive peak for the complex and a negative peak corresponding to the amount of hFc removed from the running buffer for complex formation. From the retention time of the complex, its molecular mass (70 kDa), i.e., its stoichiometry (1:1), was estimated (Figure 2b), and from the integral of the negative peak, the amount of hFc used for complex formation with sFcγRIIa was determined; 120 μg of injected sFcγRIIa was complexed with 221 μg of hFc which corresponds to a 1.2:1 molar ratio. A similar result pointing to a 1:1 stoichiometry was obtained for sFcγRIIb (data not shown).

Because of the large excess of hFc in this experimental setup, it cannot be excluded that more than one sFcγRII can bind to one hFc. Thus, in a second set of experiments, a HPLC size exclusion column was equilibrated with sFcγRIIa. The injected sample contained a fixed amount of hFc complemented with additional sFcγRIIa. Independent of the injected hFc:sFcγRIIa ratio, a uniform complex peak was recorded with a retention time of 58 min (Figure 3a). Depending on the amount of sFcγRIIa co-injected, a second peak is observed. The integral of that peak is positive,

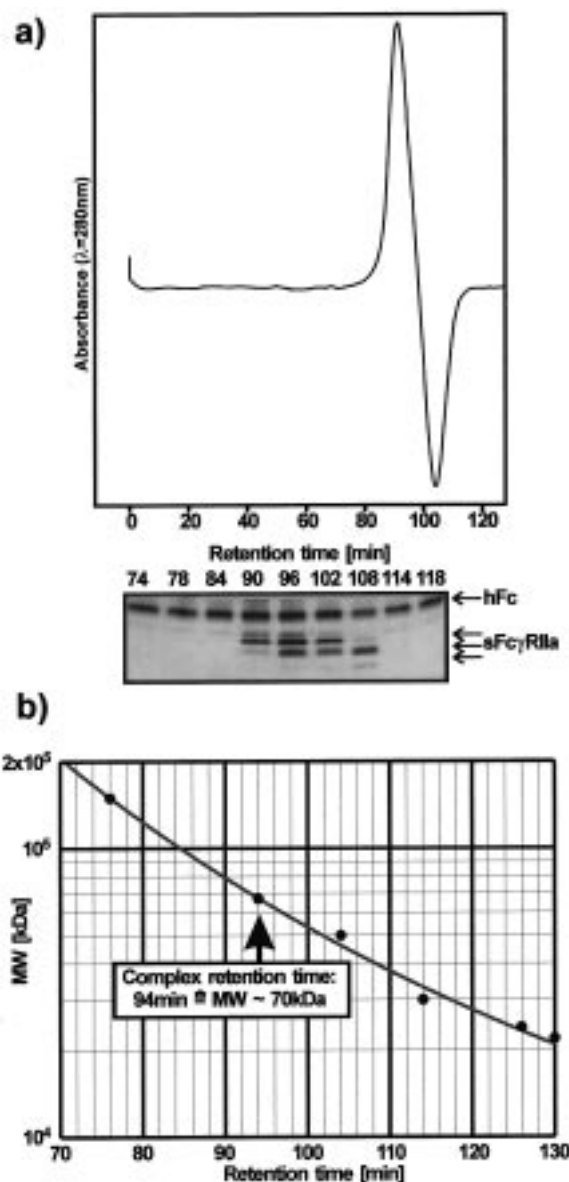


FIGURE 2: Determination of sFc $\gamma$ RII:hFc stoichiometry. (a) sFc $\gamma$ RIIa solved in equilibration buffer containing hFc was applied to a size-exclusion chromatography column and the absorbance of the effluent measured (280 nm). (Gel) Silver-stained 15% SDS-PAGE with 10  $\mu$ L samples taken from the column effluent at the indicated retention times. (b) The molecular sieve column was calibrated with proteins of known size [hIgG, 150 kDa; BSA, 67 kDa; hFc, 50 kDa; Fc $\gamma$ RIIa (BHK21-derived), 30 kDa; Fc $\gamma$ RIIa (SF9-derived), 22 kDa; lysozyme, 14 kDa] and the molecular weight of the complex estimated.

corresponding to an excess, or negative, corresponding to a lack of sFc $\gamma$ RIIa used for complex formation, which is in the latter case removed from the running buffer ( $t = 70$  min). The integral of the sFc $\gamma$ RIIa peak decreases when the correct stoichiometry between the complex constituents is approached (Figure 3a, curve 3). When sFc $\gamma$ RIIa and hFc are injected in 2.7:1 stoichiometry, the integral of the second peak is found to be near zero. Accordingly, injection of a 0:1 (Figure 3a, curve 1) or a 8:1 ratio (Figure 3a, curve 2) resulted in relative integrals of  $-2.4$  or  $4.9$  which points to a 2:1 stoichiometry of the sFc $\gamma$ RIIa:hFc complex under these conditions (Figure 3b). Taken together, the experiments shown in Figure 2 and Figure 3 indicate that hFc can bind one or two sFc $\gamma$ RII molecules (Figure 3c).

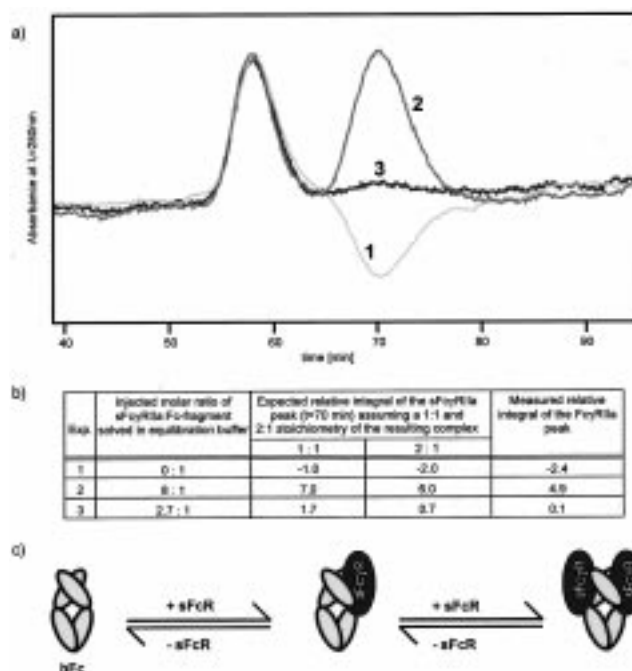


FIGURE 3: Titration of sFc $\gamma$ RIIa:hFc complex stoichiometry. The stoichiometry of sFc $\gamma$ RIIa:hFc was determined on a size exclusion chromatography column equilibrated with the soluble receptor. (a) A constant amount of hFc was mixed with different molar ratios of sFc $\gamma$ RIIa and applied to the column, and the elution profile was recorded (denoted as experiments 1–3). (b) Comparison of the measured and the expected relative integrals of the sFc $\gamma$ RIIa:hFc complex assuming a 1:1 or 2:1 stoichiometry. The integral of the sFc $\gamma$ RIIa peak ( $t = 70$  min), which reveals the amount of sFc $\gamma$ RIIa used for complexation, was measured for the three experiments (Exp. 1–3). The measured integrals were converted to molar amounts of sFc $\gamma$ RIIa and related to the molar amount of hFc injected. (c) According to the experiments depicted in Figures 2 and 3, the sFc $\gamma$ RII:hFc complex can exist in a 1:1 and a 2:1 stoichiometry.

**Determination of the Dissociation Constant of the sFc $\gamma$ RIIa:hFc Complex.** The dissociation constant of the sFc $\gamma$ RIIa:hFc complex in a cell- and membrane-free system was determined by fluorescence titration. With this method, the actual dissociation constant is directly accessible but a rather high background correction has to be tolerated. In the case of the titration with sFc $\gamma$ RIIa, the fluorescence difference signal was 19% below the total recorded fluorescence intensity and was too small in the case of sFc $\gamma$ RIIb for determination of the dissociation constant. To give an impression of the reliability of the method, Figure 4 shows three independent experiments with two different hFc concentrations. A parabolic curve according to the function given under Materials and Methods was fitted to the data, and the dissociation constant of the sFc $\gamma$ RIIa:hFc complex was determined to  $(2.5 \times 10^{-7}) \pm (0.3 \times 10^{-7})$  M.

**Inhibition of Immunocomplex Binding to B Cells.** One major characteristic of sFc $\gamma$ R is their immunosuppressive potential. Due to the competitive binding of sFc $\gamma$ R and the cell-bound Fc $\gamma$ R to immunocomplexes, the effector functions of the respective cells are inhibited.

The capability of the two recombinant receptors to block immunocomplex recognition by B cells was tested. Therefore, constant amounts of B cells and a hIgG simulating the immunocomplexes were incubated with varying amounts of sFc $\gamma$ RII isoforms, and the residual amount of immunocom-

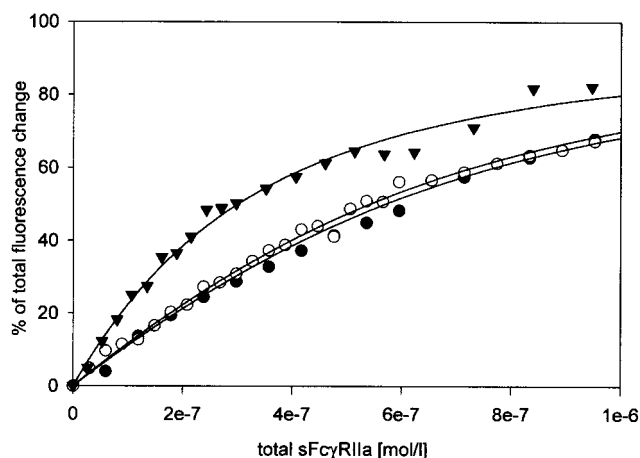


FIGURE 4: Determination of the dissociation constant of the sFcγRIIa:hFc complex. The formation of the sFcγRIIa:hFc complex is accompanied by a fluorescence change, which is depicted as percent of the total fluorescence change ( $\Delta F_{\max}$ ) versus concentration of sFcγRIIa. Therefore, a  $1.68 \times 10^{-7}$  M (▼) or a  $5.59 \times 10^{-7}$  M (●, ○) solution of the hFc was titrated with sFcγRIIa. The dissociation constants were obtained by fitting the equation derived from the law of mass effects to the data. The independent experiments resulted in three dissociation constants of  $(2.2 \times 10^{-7}) \pm (0.2 \times 10^{-7})$  M (▼),  $(2.9 \times 10^{-7}) \pm (0.4 \times 10^{-7})$  M (●), and  $(2.6 \times 10^{-7}) \pm (0.4 \times 10^{-7})$  M (○) with the respective standard errors. Note that the initial gradient of curve (▼) is much steeper than the gradient of the other curves and saturation is earlier approached due to the lower concentration of hFc in the experiment.

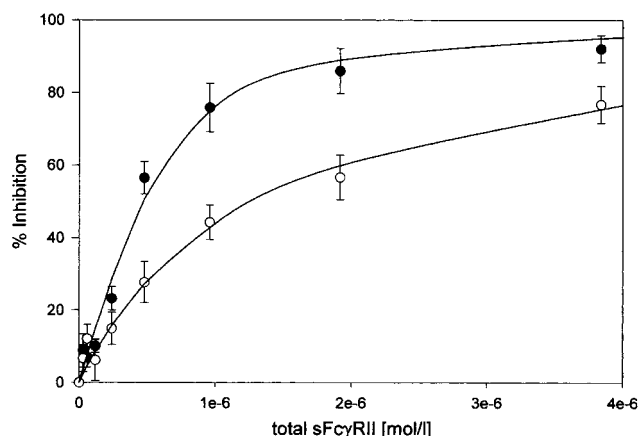


FIGURE 5: Inhibition of immunocomplex binding to B cells by sFcγRII isoforms. aIgG was preincubated with different concentrations of sFcγRIIa (●) or sFcγRIIb (○) and added to human B cells. The percent inhibition values were determined as described and plotted against the receptor concentration in the experiment. The error bars represent the standard deviation from four independent measurements. The dissociation constants were obtained by fitting  $(1.7 \times 10^{-7}) \pm (0.6 \times 10^{-7})$  M (FcγRIIa) and  $(1.4 \times 10^{-6}) \pm (0.5 \times 10^{-6})$  M (FcγRIIb), with the standard error indicated.

plexes bound to the B cells (Daudi) was measured by FACS analysis (Figure 5).

From these data,  $IC_{50}$  values for sFcγRIIa ( $IC_{50} = 0.5 \times 10^{-6}$  M) and sFcγRIIb ( $IC_{50} = 1.3 \times 10^{-6}$  M) were determined. Additionally, a similar function used for the evaluation of the fluorescence titration experiment was fitted to the data, and the resulting apparent dissociation constants for sFcγRIIa [ $K_D = (1.7 \times 10^{-7}) \pm (0.6 \times 10^{-7})$  M] and sFcγRIIb [ $K_D = (1.4 \times 10^{-6}) \pm (3 \times 10^{-7})$  M] were calculated (Figure 5).

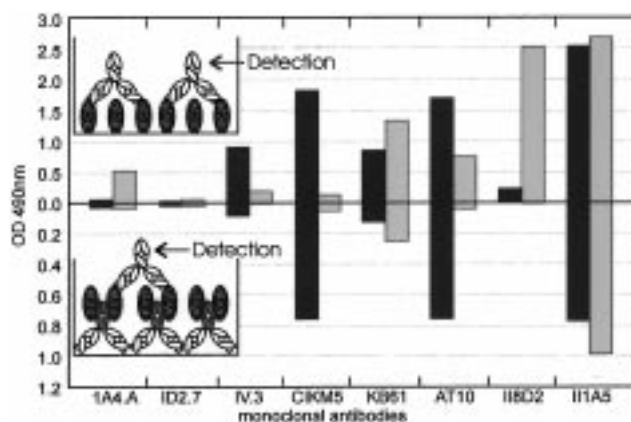


FIGURE 6: Isoform specificity of anti-CD32 mAbs. Microtiter plates coated with sFcγRIIa (black bars) and sFcγRIIb (gray bars) were incubated with anti-CD32 mAbs. Binding was quantified with a peroxidase-labeled secondary antibody (upper part). The ability of the anti-CD32 mAbs to bind to the IgG binding site of sFcγRII molecules was tested in a second assay (lower part). sFcγRII isoforms were bound to precoated hIgG employing their IgG binding capability. After incubation with anti-CD32 mAbs and washing, the residual bound mAbs were quantified as described in the upper part.

**Characterization of Anti-CD32 mAbs with sFcγRII Isoforms.** We established an ELISA through which the affinity of different anti-CD32 mAbs to sFcγRII isoforms could be quantified. Moreover, in a modification of the assay, we are able to identify anti-CD32 mAbs that inhibit the binding of sFcγRIIs to IgG. While mAbs IV.3, CIK5, and AT10 preferentially bind to sFcγRIIa, the opposite is the case for 1A4.A, KB61, and II8D2. II1A5 recognizes both isoforms (Figure 6). mAbs that interfere with the recognition of IgG by the FcγRIIs are 1A4.A, IV.3, and II8D2. The linear epitopes for 1A4.A, II8D2, and II1A5 are known (31). While 1A4.A was raised against amino acid residues 27–36 of sFcγRIIb, the epitopes of II1A5 and II8D2 are residues 50–56 and 132–138 of sFcγRIIb, respectively. The regions involved in IgG binding were identified through mutagenesis studies (40–42) and consist mainly of three regions corresponding to residues 109–116 (B/C loop), 130–135 (C'/E loop), and 154–161 (F/G loop) of sFcγRIIb. While the decreased binding of 1A4.A to the complexed receptor may be explained by steric hindrance of the large IgM, the nonbinding II8D2 confirmed an involvement of the C'/E loop in IgG binding.

**Crystallization and Preliminary Crystallographic Results.** The crystallization of sFcγRII was performed in sitting drops with a sparse matrix screening approach using the vapor diffusion method. Initial crystals of both sFcγRIIa and sFcγRIIb could be improved to yield three-dimensional single crystals that were suitable for X-ray crystallography. While the sFcγRIIa crystals were multiple-twinned, the sFcγRIIb isoform yielded single crystals that grew from a mixture of the protein solution with the reservoir solution (0.1 M MES/NaOH, 0.2 M magnesium acetate, 28% PEG 8000, 2.5% 1,4-dioxane, pH 5.3) within a period of 2 months. The resulting crystals of size  $0.1 \text{ mm} \times 0.1 \text{ mm} \times 0.04 \text{ mm}$  diffracted X-rays to a resolution of  $3.0 \text{ \AA}$ , and a complete data set was recorded (Table 2). The unit cell contained one molecule in the asymmetric unit which leads to an estimated solvent content of 44%. The structure solution is in progress and must be performed with the method of multiple isomor-



Table 2: Diffraction Data Statistics Obtained from sFcγRIIb Crystals

space group	<i>P</i> 3 <sub>1</sub> 21 [152]
unit cell dimension	<i>a</i> = <i>b</i> = 50.6 Å, <i>c</i> = 119.9 Å, $\alpha = \beta = 90^\circ$ , $\gamma = 120^\circ$
<i>R</i> <sub>merge</sub> <sup>a</sup>	13.0%
resolution	3.0 Å
unique reflections	3545
completeness	93.0%
multiplicity	2.5
<i>V</i> <sub>M</sub>	2.22 Å <sup>3</sup> , 1 molecule per asymmetric unit, 44% solvent content

$$^a R_{\text{merge}} = \sum |I_h - \langle I_h \rangle| / \sum \langle I_h \rangle$$

phous replacement (MIR) since a structure solution employing the method of molecular replacement using domains of the human IgG1 Fc fragment (43) as search model failed.

## DISCUSSION

**Biochemical Characterization.** In this report we describe a method to produce and purify recombinant active human sFcγRII. For several years the baculovirus expression system gained importance in the production of recombinant proteins. The advantages of this system are high yields and a short contact time of the product with the culture medium which reduces the risk of proteolysis. Adverse in this context is the rather low glycosylation of the protein which might influence the function of the molecule. A striking example is the Fc part of IgG which loses several functions when the glycosylation is removed (44). However, we could demonstrate that the N-glycosylation of sFcγRII is not essential for the binding to IgG. This is in agreement with results obtained by Galon for the (homologous) human sFcγRIII expressed in mammalian cells. In this protein, the carbohydrates represent nearly 50% of the protein, and it was shown that the glycosylation exerts only a minor influence on the binding of the receptor to IgG (45).

The determination of the stoichiometry led to an interesting result. Although the interest in the IgG binding site of FcγRs has been investigated for many years (40–42, 44, 46–48), the stoichiometry of the complex is still unclear. We have shown that IgG is capable of binding two sFcγRII molecules probably by utilization of its 2-fold symmetry. These results are in contrast to those obtained by Ghirlando et al., who demonstrated a 1:1 stoichiometry of the sFcγRIII:IgG complex (49). Hence, despite the high homology of both FcγRs, their binding sites are supposed to be different or the extensive glycosylation of sFcγRIII leads to steric hindrances, thereby prohibiting the binding of two receptor molecules to one IgG.

The determination of the dissociation constant for a sFcγRIIIa:hFc complex was performed for the first time in a cell- and membrane-free system. The exclusion of potentially interfering cellular components leads to an undisturbed measurement of the fluorescence change upon complex formation. In addition, no labeling of the proteins is necessary which could affect the dissociation constant. Unfortunately, the measurement could not be performed with sFcγRIIb as this molecule did not exert a fluorescence change upon complex formation. The only fluorescence active sequence difference between the two isoforms is amino acid residue 160 where the phenylalanine of FcγRIIIa is exchanged for a

tyrosine in FcγRIIb. This residue is located in the F/G loop which is partially responsible for IgG binding (41). As a fluorescence reduction in general represents a shift into a more hydrophilic ambience, this could explain why the dissociation constant of sFcγRIIb cannot be measured by this method. Y160, which contributes much more to the fluorescence than F160, will probably be in a more hydrophobic environment after binding of hFc; hence, the general fluorescence decrease might be compensated by the increased fluorescence of the tyrosine. The value of the dissociation constant with  $2.5 \times 10^{-7}$  M is lower than estimated for the membrane-bound form by other groups with  $\geq 10^{-6}$  M (40, 50, 51). The observed differences could be due to steric hindrance by the membrane in tests with entire cells. This could be demonstrated for soluble and membrane-bound FcγRII which showed a different binding characteristic for mouse IgG subclasses (52).

**Immunological Characterization.** We developed an assay that allows the determination of the inhibition of immunocomplex binding to FcγR<sup>+</sup> cells by FACS analysis. The advantage to other tests such as rosetting inhibition assays or the inhibition of the Arthus reaction (52) in animals is the practicability and reproducibility of the test. With the obtained data, even the calculation of a dissociation constant is possible. The calculated constants are denoted as apparent because the number and isoforms of the membrane-bound FcγRs are not exactly determined. Therefore, the dissociation constants of FcγRIIIa obtained through both methods may not be compared. Nevertheless, a nearly 10-fold difference between the apparent dissociation constants of the two FcγR isoforms is found under comparable conditions. This difference might be significant for triggering the effector functions of cells equipped with a different expression pattern of the two isoforms. In contrast the soluble forms of the receptors should always be saturated with IgG in vivo since the concentration of sFcγRII is around 1000-fold lower (<300 pM, 53) and the IgG concentration is 200-fold higher (50 μM) compared to the test conditions. Therefore, an influence of sFcγRII via a competitive mechanism on immunoregulation seems unlikely. During the last years, it was supposed that these soluble receptors represent a ligand for another membrane protein, eventually CR3 or CR4 (12, 14). An interaction via these molecules may represent a way in which immunosuppressive effects such as the down-regulation of antibody production (11) or the inhibition of proliferation and cytotoxic effects (23) could be explained.

We developed an ELISA assay which is capable of quantifying (a) isoform specificity and (b) binding site reactivity of anti-CD32 mAbs. Again we used a cell- and membrane-free system, excluding possible crossreactions with other proteins. Unfortunately, the glycosylation possesses a high influence on mAb binding. While both mAbs II1A5 and II8D2 show a high affinity to the Baculo- and BHK-21-derived FcγRII, they do not bind the same proteins on B cells (54). The reason for this behavior might be a different glycosylation pattern or associated proteins that exert steric hindrance to the mAb binding site.

**Crystallization of sFcγRII Isoforms.** Our crystallization trials were performed with material expressed in insect cells using recombinant baculoviruses. In contrast to a bacterial expression system, these lower eukaryotic cells perform all posttranslational modifications such as the processing of

signal peptides and the promotion of disulfide bridge formation (34). Additionally they perform only minor glycosylation compared to mammalian expression systems or yeast, therefore being the expression system of choice for crystallization trials where an extensive and unstructured carbohydrate moiety is disadvantageous. At least in the case of sFc $\gamma$ RIIb the small percentage of glycosylation, even though heterogeneous, is tolerated. The structure solution of sFc $\gamma$ RII isoforms will answer many questions concerning their binding to IgG and in addition will support or disprove postulated theories which were attributed to this point in the past.

## ACKNOWLEDGMENT

We thank Ashley Hayes for the introduction into the baculovirus expression system, Deborah Shapira for the generous gift of mAb CIKM5, Ernst-Jürgen Kanzy for the purified hFc, Rainer Beckmann for protein sequencing, John Richardson for helpful discussions, and Christoph Eckerskorn for performing the ESI-MS.

## REFERENCES

- Unkeless, J. C., Scigliano, E., and Freedman, V. H. (1988) *Annu. Rev. Immunol.* 6, 251–281.
- Fridman, W. H., Bonnerot, C., Daeron, M., Amigorena, S., Teillaud, J.-L., and Sautès, C. (1992) *Immunol. Rev.* 125, 49–76.
- Gergely, J., Sármay, G., and Rajnavölgyi, E. (1992) *Crit. Rev. Biochem. Mol.* 27, 191–225.
- van de Winkel, J. G. J., and Capel, P. J. A. (1993) *Immunol. Today* 14, 215–221.
- Fridman, W. H., and Golstein, P. (1974) *Cell. Immunol.* 11, 442–455.
- Calvo, C. F., Watanabe, S., Métivier, D., and Senik, A. (1986) *Eur. J. Immunol.* 16, 25–30.
- Sautès, C., Varin, N., Teillaud, C., Daeron, M., Even, J., Hogarth, P. M., and Fridman, W. H. (1991) *Eur. J. Immunol.* 21, 231–234.
- Bazil, V., and Strominger, J. L. (1994) *J. Immunol.* 152, 1314–1322.
- Rappaport, E. F., Cassel, D. L., Walterhouse, D. O., McKenzie, S. E., Surrey, S., Keller, M. A., Schreiber, A. D., and Schwartz, E. (1993) *Exp. Hematol.* 21, 689–696.
- de la Salle, C., Esposito-Farese, M.-E., Bieber, T., Moncuit, J., Morales, M., Wollenberg, A., de la Salle, H., Fridman, W. H., Cazenave, J.-P., Teillaud, J.-L., and Hanau, D. (1992) *Invest. Dermatol.* 99, 15S–17S.
- Varin, N., Sautès, C., Galinha, A., Even, J., Hogarth, P. M., and Fridman, W. H. (1989) *Eur. J. Immunol.* 19, 2263–2268.
- Zhou, M.-J., Todd, R. F., van de Winkel, J. G. J., and Petty, H. R. (1993) *J. Immunol.* 150(7), 3030–3041.
- Galon, J., Bouchard, C., Fridman, W. H., and Sautès, C. (1995) *Immunol. Lett.* 44, 175–181.
- Lynch, R. G., Hagen, M., Mueller, A., and Sandor, M. (1995) *Immunol. Lett.* 44, 105–109.
- Littaua, R., Kurane, I., and Ennis F. A. (1990) *J. Immunol.* 144, 3183–3186.
- Homsy, J., Meyer, M., Tateno, M., Clarkson, S., and Levy, J. A. (1989) *Science* 244, 1357–1360.
- Yang, Z., Delgado, R., Xu, L., Todd, R. F., Nabel, E. G., Sanchez, A., and Nabel, G. J. (1998) *Science* 279, 983–984.
- Ravanel, K., Castelle, C., Defrance, T., Wild, T. F., Charron, D., Lotteau, V., and Rabourdincombe, C. (1997) *J. Exp. Med.* 186, 269–278.
- Hutin, P., Lamour, A., Pennec, Y. L., Soubrane, C., Dien, G., Khayat, D., and Youinou, P. (1994) *Int. Arch. Allergy Immunol.* 103, 23–27.
- Ulvestad, E., Matre, R., and Tonder, O. (1988) *Scand. J. Rheumatol., Suppl.* 75, 203–208.
- Mathiot, C., Teillaud, J. L., Elmalek, M., Mosseri, L., Euler-Ziegler, L., Daragon, A., Grosbois, B., Michaux, J. L., Facon, T., Bernard, J. F., Duclos, B., Monconduit, M., and Fridman, W. H. (1993) *J. Clin. Immunol.* 13, 41–48.
- Khayat, D., Soubrane, C., Andriew, J. M., Visonneau, S., Eme, D., Tourani, J. M., Beldjord, K., Weil, M., Fernandez, E., and Jaquillat, C. (1990) *J. Infect. Dis.* 161, 430–435.
- Hoover, R. G., Lary, C., Page, R., Travis, P., Owens, R., Flick, J., Kornbluth, J., and Barlogie, B. (1995) *J. Clin. Invest.* 95, 241–247.
- Smith, G. E., Summers, M. D., and Fraser, M. J. (1983) *Mol. Cell. Biol.* 3, 2156–2165.
- Engelhardt, W., Gorczyta, H., Butterweck, A., Mönkemann, H., and Frey, J. (1991) *Eur. J. Immunol.* 21, 2227–2238.
- Vail, P. V., Sutter, G., Jay, D. L., and Gough, D. (1971) *J. Invertebr. Pathol.* 17, 383–388.
- Laemmli, U. K. (1970) *Nature* 227, 680–685.
- Looney, R. J., Abraham, G. N., and Anderson, C. L. (1986) *J. Immunol.* 136, 1641–1647.
- Greenman, J., Tutt, A. L., George, A. J. T., Pulford, K. A. F., Stevenson, G. T., and Glennie, M. J. (1991) *Mol. Immunol.* 28, 1243–1254.
- Pulford, K., Ralfkiaer, E., MacDonald, S. M., Erber, W. N., Falini, B., Gatter, K. C., and Mason, D. Y. (1986) *Immunology* 57, 71–76.
- Weinrich, V., Sondermann, P., Bewarder, N., Wissel, K., and Frey, J. (1996) *Hybridoma* 15, 109–116.
- Engelhardt, W., Geerds, C., and Frey, J. (1990) *Eur. J. Immunol.* 20, 1367–1377.
- Sanger, F., Nicklen, S., and Coulson, A. R. (1977) *Proc. Natl. Acad. Sci. U.S.A.* 74, 5463–5467.
- King, L. A., and Possee, R. D. (1992) *The Baculovirus Expression System, A Laboratory Guide*, Chapman & Hall, London, England.
- Lehmann, J., Heidemann, R., Riese, U., Lütkemeyer, D., and Büntemeyer, H. (1992) *BioEngineering* 8, 36–38.
- Gill, S. C., and von Hippel, P. H. (1989) *Anal. Biochem.* 182, 319–326.
- Hummel, J. P., and Dreyer, W. J. (1962) *Biochim. Biophys. Acta* 63, 530–532.
- Leslie, A. G. W. (1997) *Mosflm user guide, mosflm version 5.50*, MRC Laboratory of Molecular Biology, Cambridge, U.K.
- Collaborative Computational Project, Number 4 (1994) *Acta Crystallogr. D50*, 760–763.
- Hogarth, P. M., Hulett, M. D., Ierino, F. L., Tate, B., Powell, M. S., and Brinkworth, R. I. (1992) *Immunol. Rev.* 125, 21–35.
- Hulett, M. D., Witort, E., Brinkworth, R. I., McKenzie, I. F. C., and Hogarth, P. M. (1994) *J. Biol. Chem.* 269, 15287–15293.
- Hulett, M. D., Witort, E., Brinkworth, R. I., McKenzie, I. F. C., and Hogarth, P. M. (1995) *J. Biol. Chem.* 270, 21188–21194.
- Deisenhofer, J. (1981) *Biochemistry* 20, 2361–2370.
- Jefferis, R., Lund, J., and Goodall, M. (1995) *Immunol. Lett.* 44, 111–117.
- Galon, J., Robertson, M. W., Galinha, A., Mazieres, N., Spagnoli, R., Fridman, W. H., and Sautès, C. (1997) *Eur. J. Immunol.* 27, 1928–1932.
- Burton, D. R., Jefferis, R., Partridge, L. J., and Woof, J. M. (1988) *Mol. Immunol.* 25, 1175–1181.
- Hibbs, M. L., Tolvanen, M., and Carpen, O. (1994) *J. Immunol.* 152, 4466–4474.
- Tamm, A., Kister, A., Nolte, K. U., Gessner, J. E., and Schmidt, R. E. (1996) *J. Biol. Chem.* 271, 3659–3666.
- Ghirlando, R., Keown, M. B., Mackay, G. A., Lewis, M. S., Unkeless, J. C., and Gould, H. J. (1995) *Biochemistry* 34, 13320–13327.
- Stengelin, S., Stamenkovic, I., and Seed, B. (1988) *EMBO J.* 7, 1053–1059.



51. Warmerdam, P. A. M., van de Winkel, J. G. J., Gosselin, E. J., and Capel, P. J. A. (1990) *J. Exp. Med.* 172, 19–25.
52. Ierino, F. L., Powell, M. S., McKenzie, I. F. C., and Hogarth, P. M. (1993) *J. Exp. Med.* 178, 1617–1628.
53. Astier, A., de la Salle, H., Moncuit, J., Freund, M., Cazenave, J.-P., Fridman, W.-H., Hanau, D., and Teillaud, J.-L. (1993) *J. Immunol. Methods* 166, 1–10.
54. Budde, P., Weinrich, V., Sondermann, P., Bewarder, N., Kilian, A., Schulzeck, O., and Frey, J. (1995) in *Leucocyte Typing V, Cell Differentiation Antigens* (Schlossman, S. F., Ed.) pp 828–832, Oxford University Press, England.

BI982889Q